ELSEVIER

Chemical Engineering Science 60 (2005) 337–345

Chemical Engineering Science

www.elsevier.com/locate/ces

Numerical simulation for diffusion of matter in compound round jet by three-dimensional particle method

Tomomi Uchiyama[a,*], Akihito Ichikawa[b]

[a] *ECOTOPIA Science Research Institute, Nagoya University, Furo-cho, Chikusa-ku, Nagoya 464-8603, Japan*
[b] *Toyota Motor Corporation Toyota-Cho, Toyota 471-8571, Japan*

Received 1 December 2003; received in revised form 24 July 2004; accepted 25 July 2004
Available online 29 September 2004

Abstract

A three-dimensional particle method for the diffusion of matter in a round jet is proposed. The flow field is calculated with a vortex method, whereas the concentration field is simulated through a method analogous to the vortex method. The particle method is based on the Lagrangian approach; thus no computational grids are needed. It is applied to simulate the diffusion of matter in a compound round jet. The large-scale eddies, appearing just downstream of the disappearing point of the potential core, cause the diffusion of matter in the radial direction. In the subsequent developed region of the velocity field, the diffusion proceeds to the smaller vortical structure. The mean concentration and the concentration fluctuation intensity are in the self-preservation state at $x/D \geqslant 8$ and $x/D \geqslant 13$, respectively. These numerical results are favorably compared with experimental ones, indicating that the present particle method is usefully employed to simulate the diffusion of matter in a round jet.

Keywords: Numerical analysis; Diffusion; Fluid mechanics; Environment; Jet; Lagrangian method

1. Introduction

The diffusion of matter in turbulent flow is frequently observed in various industrial equipment, such as reactors and combustors, as well as in the ocean and atmosphere. Therefore, the development of the numerical method that can accurately predict the diffusion of matter has been earnestly demanded in engineering and environmental sciences. A number of numerical methods have thus far been proposed, and valuable results on the DNS (Riley and Metcalfe, 1985) and LES (Cook and Riley, 1994) have been accumulated.

On the other hand, attention has been given to particle methods because they can numerically analyze the motion of matter with various spatial and temporal scales, such as nebula, plasma and fluid (Hockney and Eastwood, 1985). In these methods, the behavior of small particles having a physical property, such as mass, electric charge or vorticity, is calculated by the Lagrangian approach and the whole motion of the matter is simulated on the basis of behavior of each particle. The methods do not need the computational grid which is indispensable to the finite difference method and the finite element method. Moreover, the numerical stability is quite high because the computation is chiefly composed of numerical integrations.

The particle method for fluid simulation is called the vortex method, and it has been usefully applied to calculate free turbulent flows, in which the organized large-scale eddies play a dominant role in the development and momentum transfer of the flow (Leonard, 1980). This is because the methods can directly simulate the development of a vortex structure, such as the formation and deformation of vortices, by calculating the behavior of vortex elements through the Lagrangian method. The vortex methods have been widely applied to various flow phenomena recently, and the applicability is gradually being extended. The authors (Uchiyama

* Corresponding author. Tel./fax: +81-52-789-5187.
E-mail address: uchiyama@info.human.nagoya-u.ac.jp (T. Uchiyama).

0009-2509/$ - see front matter © 2004 Elsevier Ltd. All rights reserved.
doi:10.1016/j.ces.2004.07.119

and Naruse, 2001) have proposed a vortex method for free turbulent flow laden with small solid particles. The method has been successfully employed for the calculation of flow around a circular cylinder (Uchiyama et al., 2000), a mixing layer (Uchiyama and Naruse, 2002), a slit nozzle jet (Uchiyama and Naruse, 2003), and a wake (Uchiyama and Yagami, 2003). In the succeeding study (Uchiyama, 2004), the method was applied to calculate the particulate jet induced by free-falling particles in a quiescent air, and the effects of the particle diameter and density on the entrained air flow rate were successfully simulated.

A transport equation for vorticity is solved in the vortex method, while an equation of the same type, i.e. a diffusion equation, governs the diffusion of matter and heat. Therefore, numerical methods based on the calculating procedure of the vortex method have so far been proposed to solve the diffusion equation (Ogami, 2001; Kamemoto and Miyasaka, 2000). By using such a particle method, the authors (Uchiyama and Okita, 2003) simulated a point-source plume diffusion field of matter on the flow around a circular cylinder. The flow field was solved by the vortex method, and the diffusion field was calculated through the method analogous to the vortex method. The simulation demonstrated that the diffusing matter is entrained into the Karman vortices in accordance with the corresponding experiment. The mean concentration and fluctuation intensity were also favorably compared with the measured results. The particle method was also applied to calculate a plane mixing layer (Otsuki et al., 2002), and the mixing asymmetry due to the large-scale eddies was successfully simulated. But the three-dimensional simulation for diffusion of matter by the particle method has not been carried out.

The experimental studies on the diffusion of matter in free turbulent flows, e.g. a mixing layer (Breidenthal, 1981) and circular jets (Hasegawa et al., 1991; Yamashita et al., 1996), elucidated that the concentration distribution is markedly governed by the three-dimensional vortical structure. Thus, the three-dimensional particle method, which has a higher applicability to free turbulent flows, promises to be successfully used to simulate the diffusion of matter in free turbulent flow.

This study presents a three-dimensional particle method for the diffusion of matter in jet and searches for its applicability. As the flow field, a jet issuing from a round nozzle into the same fluid co-flowing is chosen, because the flow has been analyzed with a three-dimensional vortex method by the author (Uchiyama, 2003). The diffusion of the matter from the nozzle is simulated. It is shown that the simulated concentration distribution yielded by the three-dimensional vortical flow is in good agreement with the experimental one obtained by flow visualization. The mean and fluctuation concentrations are confirmed to be in the self-preservation state. These demonstrate the validity of the three-dimensional particle method for the diffusion of matter in a round jet.

2. Basic equations

2.1. Conservation equations

Assuming an incompressible flow, the conservation equations for the mass and momentum are expressed as follows:

$$\nabla \cdot \boldsymbol{u} = 0, \tag{1}$$

$$\frac{\partial \boldsymbol{u}}{\partial t} + (\boldsymbol{u} \cdot \nabla)\boldsymbol{u} = -\frac{1}{\rho}\nabla p + \nu \nabla^2 \boldsymbol{u}, \tag{2}$$

where ν is the kinematic viscosity.

When taking the curl of Eq. (2) and substituting Eq. (1) into the resulting equation, the vorticity equation is derived:

$$\frac{\partial \boldsymbol{\omega}}{\partial t} + (\boldsymbol{u} \cdot \nabla)\boldsymbol{\omega} = (\boldsymbol{\omega} \cdot \nabla)\boldsymbol{u} + \nu \nabla^2 \boldsymbol{\omega}. \tag{3}$$

The conservation equation for the concentration of matter γ is expressed as

$$\frac{\partial \gamma}{\partial t} + (\boldsymbol{u} \cdot \nabla)\gamma = \kappa \nabla^2 \gamma, \tag{4}$$

where κ is the diffusivity. The conservation equations for the vorticity and concentration, Eqs. (3) and (4), are rewritten in the Lagrangian co-ordinates as follows:

$$\frac{\mathrm{d}\boldsymbol{\omega}}{\mathrm{d}t} = (\boldsymbol{\omega} \cdot \nabla)\boldsymbol{u} + \nu \nabla^2 \boldsymbol{\omega}, \tag{5}$$

$$\frac{\mathrm{d}\gamma}{\mathrm{d}t} = \kappa \nabla^2 \gamma. \tag{6}$$

In vortex methods, the vorticity field, discretized into vortex elements, is computed on the basis of the behavior of the elements, which is obtained from the Lagrangian calculation of Eq. (5) (Leonard, 1980). When a two-dimensional field is simulated, the first term on the right side of Eq. (5) is zero and Eq. (5) becomes the same as Eq. (6). Therefore, some numerical methods analogous to vortex methods have been applied to solve the diffusion field. In such a particle method, the diffusion field, discretized into elements, is analyzed by computing the behavior of the elements with the Lagrangian approach. By using such a two-dimensional particle method, the authors have simulated a point-source plume diffusion field of matter on the flow around a circular cylinder (Uchiyama and Okita, 2003), and they have also analyzed the mixing phenomena of matter in a plane mixing layer (Otsuki et al., 2002). In this study, a three-dimensional particle method for Eqs. (5) and (6) is proposed, and it is applied to calculate the diffusion of matter in a compound round jet.

2.2. Discretization of vorticity field

For the analysis of the compound round jet, a three-dimensional vortex method proposed in a previous paper (Uchiyama, 2003) is employed. A blob model is used for the

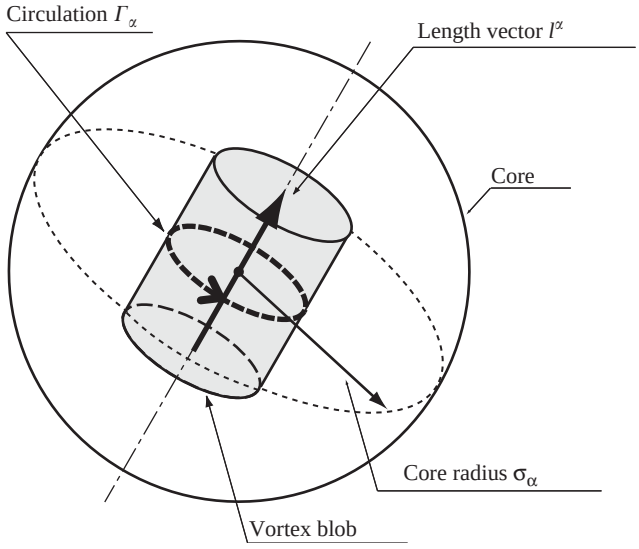

Fig. 1. Vortex element.

vortex element discretizing the vorticity field (Winckelmans and Leonard, 1993). The vortex element has a cylindrical shape as illustrated in Fig. 1, while the vorticity distribution is spherical with a finite core radius.

When the vortex element i at $\boldsymbol{x}^i$ is supposed to have the core radius σ_i, the vorticity at $\boldsymbol{x}$ induced by the element is expressed as

$$\boldsymbol{\omega}^i(\boldsymbol{x}) = \frac{\boldsymbol{\alpha}^i}{\sigma_i^3} f\left(\frac{|\,\boldsymbol{x}-\boldsymbol{x}^i\,|}{\sigma_i}\right), \tag{7}$$

where $f(\varepsilon)$ is the core distribution function, and $\boldsymbol{\alpha}^i$ the strength of the vortex element. Denoting the representative vorticity and the circulation as $\boldsymbol{\omega}^i$ and Γ_i, respectively, $\boldsymbol{\alpha}^i$ is determined by

$$\boldsymbol{\alpha}^i = \boldsymbol{\omega}^i \delta v_i = \Gamma_i \boldsymbol{l}^i, \tag{8}$$

where δv_i and $\boldsymbol{l}^i$ are the volume and length vector of the vortex element, respectively, as indicated in Fig. 1.

The following equation is used for $f(\varepsilon)$, which gives the spherical distribution of vorticity:

$$f(\varepsilon) = \frac{3}{4\pi}\exp(-\varepsilon^3). \tag{9}$$

When the vorticity field is discretized into a set of N vortex elements, the velocity $\boldsymbol{u}(\boldsymbol{x})$ is expressed by the following equation derived from Eq. (7) and Biot–Savart equation:

$$\boldsymbol{u}(\boldsymbol{x}) = -\frac{1}{4\pi}\sum_{i=1}^{N}\frac{(\boldsymbol{x}-\boldsymbol{x}^i)\times\boldsymbol{\alpha}^i}{|\,\boldsymbol{x}-\boldsymbol{x}^i\,|^3} g\left(\frac{|\,\boldsymbol{x}-\boldsymbol{x}^i\,|}{\sigma_i}\right) + \boldsymbol{u}_p, \tag{10}$$

where $\boldsymbol{u}_p$ is the potential velocity, and $g(\varepsilon)$ is determined by

$$g(\varepsilon) = 4\pi\int_0^\varepsilon f(\rho)\rho^2\,\mathrm{d}\rho. \tag{11}$$

The vortex element convects with the fluid velocity at its center. The Lagrangian method is applied to calculate the convection. It should be noted that the vorticity varies with the lapse of time owing to the change in the length of the vortex element and the viscous diffusion, as found from Eq. (5). These variations are simultaneously computed with the Lagrangian calculation for the convection of the vortex element through the following method.

The effect of viscosity v on the vorticity is simulated by a core-spreading method (Leonard, 1980), in which the core radius of vortex element σ_i is made to increase with the lapse of time.

$$\frac{\mathrm{d}\sigma_i^2}{\mathrm{d}t} = 4v. \tag{12}$$

The time evolution in vorticity owing to the stretch and contraction of the vortex element is computed with the time rate of change in the strength of vorticity $\boldsymbol{\alpha}^i$, which is derived by substituting Eqs. (7) and (10) into Eq. (5):

$$\frac{\mathrm{d}\boldsymbol{\alpha}^i}{\mathrm{d}t} = \frac{1}{4\pi}\sum_j\frac{1}{\sigma_j^3}\left\{-\frac{g(\rho)}{\rho^3}\boldsymbol{\alpha}^i\times\boldsymbol{\alpha}^j + \frac{1}{\sigma_j^2}\left[-\frac{1}{\rho}\frac{\mathrm{d}}{\mathrm{d}\rho}\left(\frac{g(\rho)}{\rho^3}\right)\right] \times[\boldsymbol{\alpha}^i\cdot(\boldsymbol{x}^i-\boldsymbol{x}^j)][(\boldsymbol{x}^i-\boldsymbol{x}^j)\times\boldsymbol{\alpha}^j]\right\}, \tag{13}$$

where $\rho = |\,\boldsymbol{x}^i-\boldsymbol{x}^j\,|/\sigma_j$, and the viscous diffusion term is neglected because it is already considered in the core-spreading method.

2.3. Discretization of concentration field

The concentration field is discretized into elements. It is postulated that each element has a finite core and that the concentration distribution within the element is expressed with a Gaussian curve. When the element j at $\boldsymbol{x}^j$ is supposed to have a core radius ε_j, the concentration at $\boldsymbol{x}$ yielded by the element is written as

$$\gamma^j(\boldsymbol{x}) = \frac{C_j}{\varepsilon_j^3} f\left(\frac{|\,\boldsymbol{x}-\boldsymbol{x}^j\,|}{\varepsilon_j}\right), \tag{14}$$

where C_j is the strength of the element, and f is given by Eq. (9).

The concentration element convects with fluid velocity at its center. The Lagrangian method is applied to calculate the convection. To consider the diffusion term of Eq. (6), the core-spreading method is also employed according to prior studies (Otsuki et al., 2002; Uchiyama and Okita, 2003).

$$\frac{\mathrm{d}\varepsilon_j^2}{\mathrm{d}t} = 4\kappa. \tag{15}$$

If the concentration field is discretized into a set of M concentration elements, the concentration $\gamma(\boldsymbol{x})$ at $\boldsymbol{x}$ is given

as follows:

$$\gamma(\boldsymbol{x}) = \sum_{j=1}^{M} \gamma_j(\boldsymbol{x}). \tag{16}$$

3. Calculating conditions

The simulation is performed on a jet issuing with velocity U_0 from a round nozzle of diameter D into the same fluid co-flowing with velocity U_a. The jet is entrained with a diffusing matter. The nondimensional numbers are set as follows: the Reynolds number $U_0 D/\nu = 2 \times 10^4$, the velocity ratio $U_a/U_0 = 0.27$, and the Schmidt number $\nu/\kappa = 1$. The flow inside the nozzle is simulated by a panel method (Uchiyama, 2003). The time step Δt is $0.1D/U_0$. The 2nd Adams–Bashforth method is applied to the Lagrangian calculation for the elements.

The vortex elements are released from the position of $x = \pi D/16$ into the flow at a time interval Δt_v $(= 2\Delta t)$, as illustrated in Fig. 2. At the release, the core radius is set at $0.4D$ and the circulation is given by the following equation:

$$\Gamma_0 = (U_0^2 - U_a^2)\Delta t_v/2. \tag{17}$$

The vorticity of the vortex element generally increases with the lapse of time in the downstream region due to the vortex stretching, causing the deterioration of the spatial resolution. To maintain the resolution, the vortex element i, of which the initial strength is $\boldsymbol{\gamma}^i$, is divided into two vortex elements having the strength $\boldsymbol{\gamma}^i/2$, when the strength becomes greater than twice its initial value (Uchiyama, 2003).

The concentration elements are released from 49 points in the nozzle exit section, as shown in Fig. 3, at a time interval Δt_c $(= 2\Delta t)$. At the release, the core radius is set at $0.4D$. The concentration γ distributes on the nozzle exit section as shown in Fig. 4, where γ_{c0} is the γ value on the jet centerline and b_γ is the half-width. The distribution is nearly represented with a Gaussian curve except near the jet periphery.

The cylindrical region downstream of the nozzle is the computational domain, of which axial length and diameter are $20D$ and $10D$, respectively. The elements leaving the domain are excluded from the calculation. To consider the exclusion of the vortex element, sink points are located $0.3D$ downstream of the domain (Uchiyama, 2003).

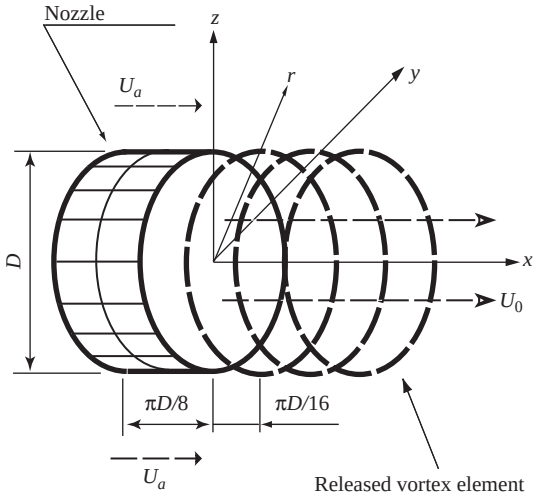

Fig. 2. Circular nozzle and released vortex element.

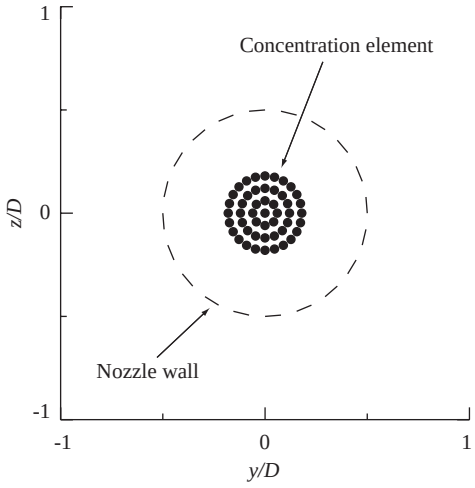

Fig. 3. Initial position of concentration element at nozzle exit.

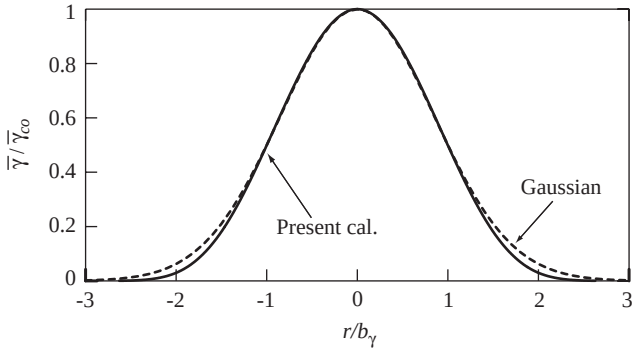

Fig. 4. Concentration distribution at nozzle exit.

4. Numerical results and discussion

4.1. Velocity field

Fig. 5 depicts the time variation for the number of vortex elements N_v in the computational domain. The N_v value slightly fluctuates around 17 300 at $t^* \geqslant 133$. This indicates that the number of vortex elements generated in the domain balances with that of vortex elements leaving the domain. Accordingly, it is found that a fully developed flow is analyzed at $t^* \geqslant 133$.

The distribution of the vortex element at $t^* = 400$ is shown in Fig. 6, where the center of each vortex element is plotted by the symbol •. The vortex elements flow straight at

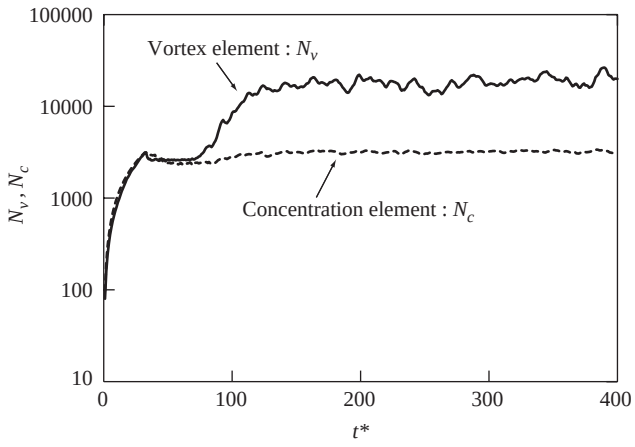

Fig. 5. Time variation of numbers of vortex elements and concentration elements.

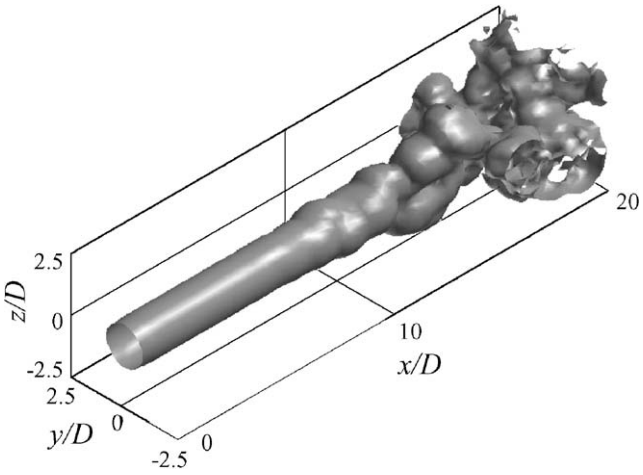

Fig. 7. Surface of constant magnitude for vorticity $|\boldsymbol{\omega}|/|\boldsymbol{\omega}_0| = 0.75$ at $t^* = 400$.

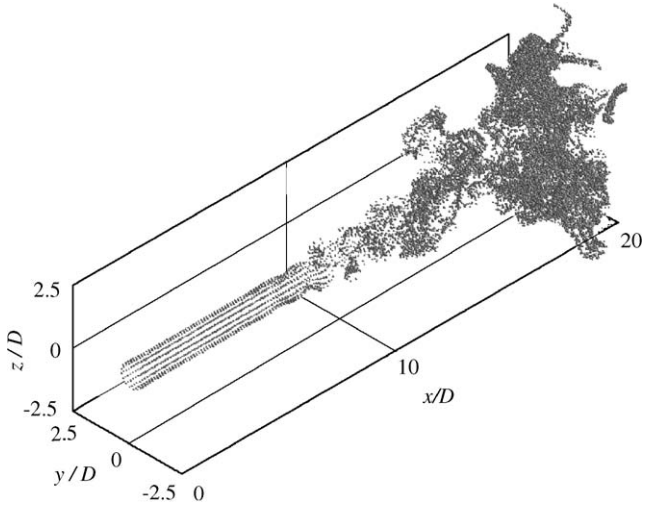

Fig. 6. Distribution of vortex element at $t^* = 400$.

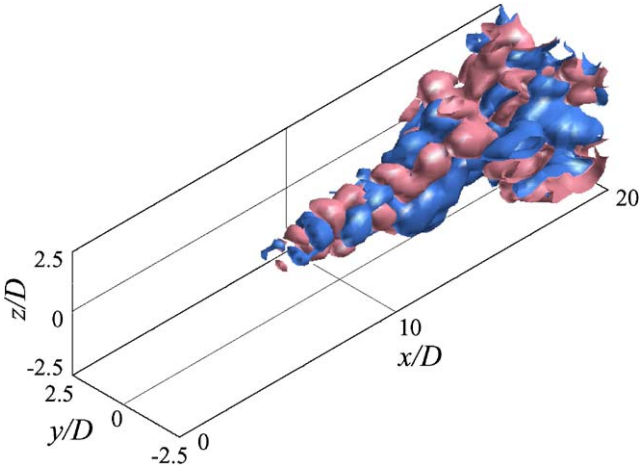

Fig. 8. Surface of constant magnitude for axial component of vorticity $|\omega_x|/|\boldsymbol{\omega}_0| = \pm 0.25$ at $t^* = 400$.

$x/D \leqslant 8$, but they immediately move in the radial direction in the downstream region. Some vortex elements form clusters. There are a lot of elements at $x/D \geqslant 14$. This is because the flow changes into the turbulent there, as discussed later, and accordingly the elements are stretched and frequently divided.

Fig. 7 shows the iso-surface for the vorticity $|\boldsymbol{\omega}|/|\boldsymbol{\omega}_0| = 0.75$ at the same instant as Fig. 6. The vorticity is calculated by taking the rotation of the velocity, and $\boldsymbol{\omega}_0$ is the vorticity at the nozzle exit. Although the vorticity distributes axisymmetrically at $x/D \leqslant 8$, such distribution decays in the downstream region. At $x/D \geqslant 11$, the flow rapidly changes into the turbulent and three-dimensional vortical structures appear.

Fig. 8 presents the iso-surfaces for the axial component of vorticity $\omega_x/\omega_0 = \pm 0.25$ at the same instant as Fig. 7. The streamwise vorticity ω_x occurs at $x/D = 6.9$. The collapse of the axisymmetrical distribution of $\boldsymbol{\omega}$ shown in Fig. 7 is due to the occurrence of ω_x. At $x/D \geqslant 8$, highly organized vortical structures are simulated, in which pairs of negative and positive vortex tubes exist and the tubes entangle. The structure of streamwise vorticity rapidly becomes finer at $x/D \geqslant 11$. Similar vortical structures have been obtained by the DNS on a slit nozzle jet (Yuu et al., 1990) and a round jet (Takeuchi et al., 1999) as well as by the vortex method for a compound round jet (Uchiyama, 2003).

The radial profile of the mean velocity U is shown in Fig. 9, where the profiles on eight sections at $8 \leqslant x/D \leqslant 15$ are plotted. According to the experiment on a compound round jet by Forstall and Shapiro (1950), the velocity U satisfies the self-preservation distribution at $x/D \geqslant 8$ and the profile is expressed with a Gaussian curve. The simulated velocity is almost in the self-preservation state and nearly approximated with the Gaussian curve. This demonstrates that the mean velocity is successfully simulated in this study.

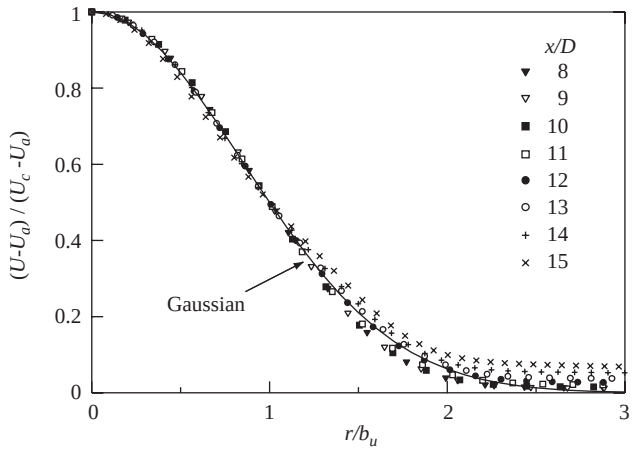

Fig. 9. Radial profile of mean axial velocity.

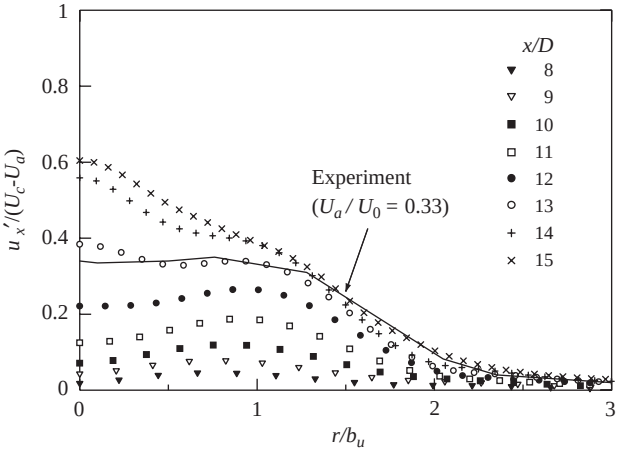

Fig. 10. Radial profile of r.m.s. axial velocity fluctuation.

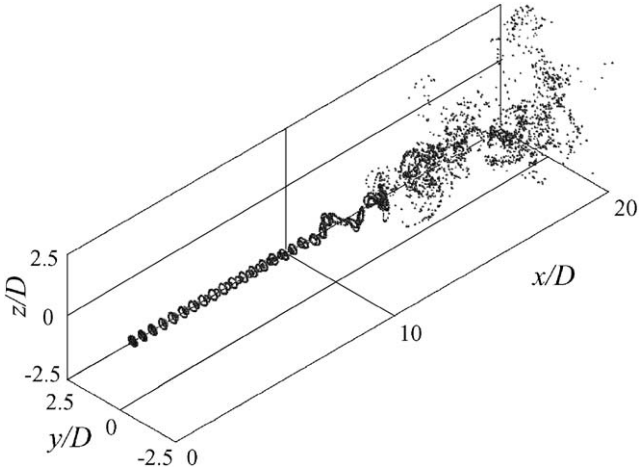

Fig. 11. Distribution of concentration element at $t^* = 400$.

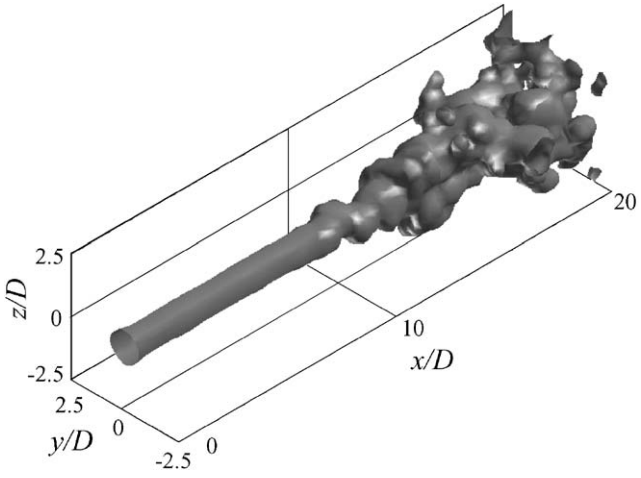

Fig. 12. Surface of constant magnitude for concentration $\gamma = 0.1$ at $t^* = 400$.

Fig. 10 shows the radial distribution of the axial component of the turbulent intensity. The nondimensional turbulent intensity heightens at $0 \leqslant r/b_u \leqslant 2.1$ with increase in the axial distance x. According to the experiment by Antonia and Bilger (1973) on jets with velocity ratios $U_a/U_0 = 0.22$ and 0.33, the nondimensional turbulent intensity increases with x at $x/D \leqslant 100$. It reaches its self-preservation state at $x/D = 152$ when $U_a/U_0 = 0.33$, as plotted by the solid line. The simulated turbulent intensity tends to approach the measured self-preservation profile at $r/b_u \geqslant 1$ with increase in x. Therefore, the present result is considered not to contradict the experimental one.

4.2. Concentration field

The time variation for the number of concentration elements N_c in the computational domain is also plotted in Fig. 5. At $t^* \geqslant 133$, N_c takes almost the constant value, and the average is 3165. It is found that a fully developed concentration field is also simulated at $t^* \geqslant 133$.

Fig. 11 presents the distribution of the concentration element at $t^* = 400$. The elements flow straight in the axial (x) direction at $x/D \geqslant 8$, where the potential core exists. In the downstream region, however, they largely disperse in the radial direction, and some elements form clusters. Such distribution is quite similar to that of the vortex element shown in Fig. 6. This is because the movements of the vortex element and concentration element convecting with the fluid velocity are computed by the Lagrangian approach.

The distribution of the concentration γ at the same instant as Fig. 11 is shown in Fig. 12, where the iso-surface of $\gamma = 0.1$ is plotted. The distribution is similar to that of the vorticity (Fig. 7), indicating that the three-dimensional vortical structure remarkably affects the concentration field.

Fig. 13(a)–(c) compares the distributions of the velocity and concentration in a x–y plane including the jet centerline, where the velocity $U_0 - U_a$ is subtracted to make the vortical flow more understandable. Distributions at three time points are depicted. The concentration γ takes its maximum

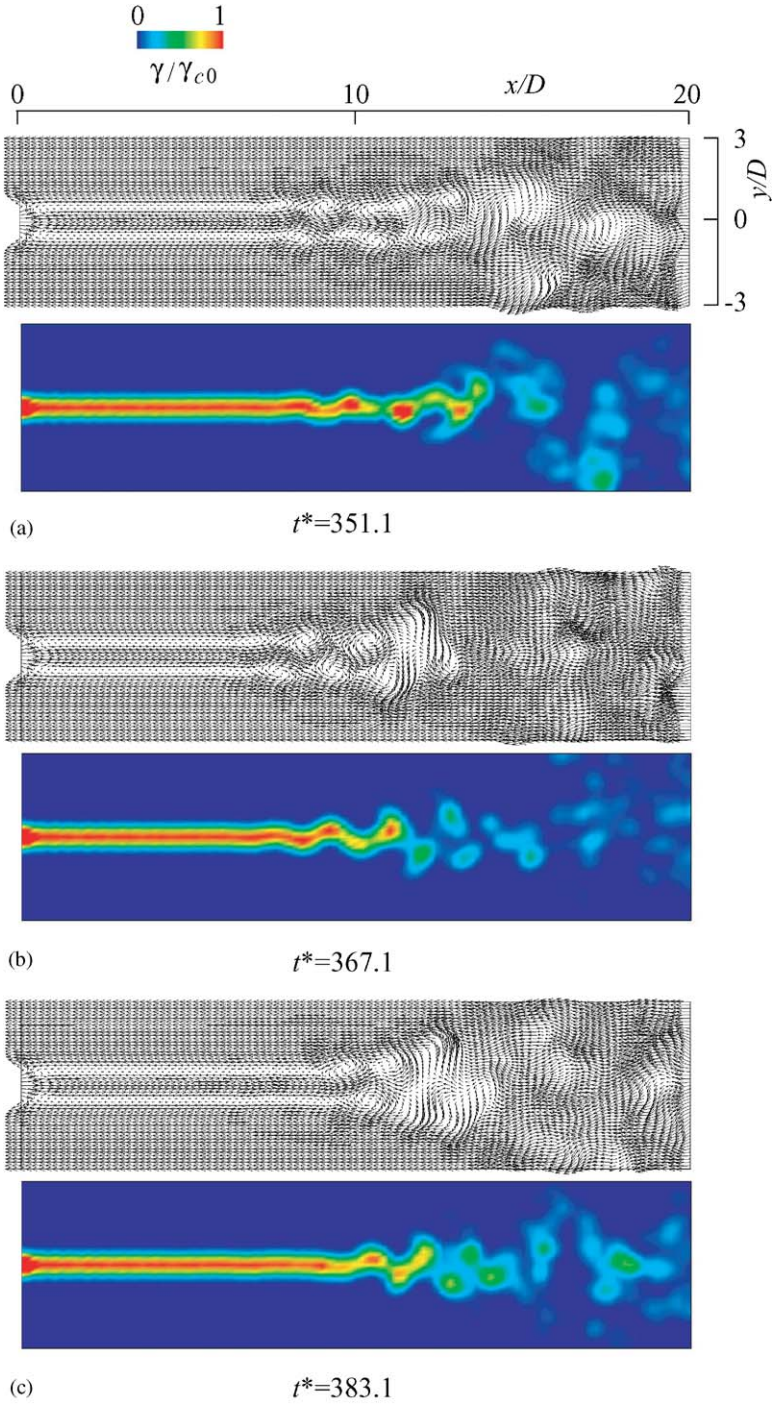

Fig. 13. (a)–(c) Distributions of velocity and concentration in x–y plane.

value on the jet centerline at $x/D \leqslant 8$, where the potential core exists, and the change in the axial (x) direction is not observable. In the downstream region ($8 \leqslant x/D \leqslant 13$), however, the large-scale eddies cause the diffusion of matter in the lateral direction, thus the concentration on the centerline drastically lowers. At $x/D \geqslant 13$, the diffusion proceeds in the smaller vortical structure. Such a role of the three-dimensional vortical structures in the diffusion of matter has also been reported by the experiments on jets (Hasegawa et al., 1991; Yamashita et al., 1996). Hasegawa et al. visualized the nitrogen jet issuing from a circular nozzle into a quiescent air, and Yamashita et al. carried out the visualization of compound round jets with the Reynolds number $U_0 D/\nu$ set at 2700 and 4800.

Fig. 14 shows the variation of concentration probability density function pdf(γ) along the jet centerline. At $x/D = 8$,

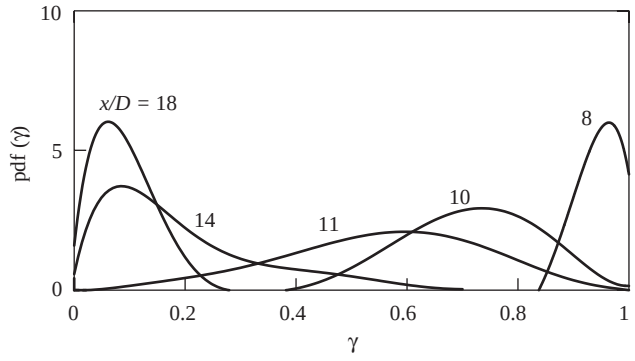

Fig. 14. Variation of concentration pdf on jet centerline in axial direction.

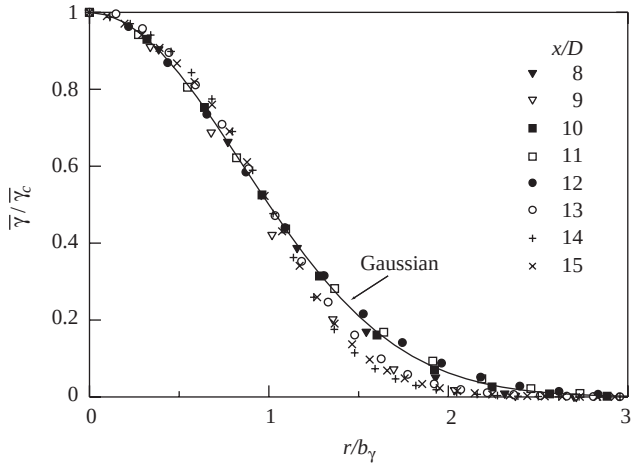

Fig. 15. Radial profile of mean concentration.

where the potential core disappears, pdf(γ) concentrates in the vicinity of unity ($\gamma = 1$). This is because the diffusion hardly occurs at $x/D \leqslant 8$, as seen in Fig. 13. In the downstream region ($x/D = 10$, 11), however, pdf(γ) distribution broadens due to the active mixing caused by the large-scale eddies. At $x/D \geqslant 14$, the pdf(γ) distribution becomes more concentrated with the peak location shifted towards the linear side. This is because the diffusion proceeds to the smaller vortical structure, as found in Fig. 13. The above-mentioned variation of the concentration pdf in the axial direction has also been revealed by the experiment on a compound round jet by Yamashita et al. (1996).

The mean concentration $\overline{\gamma}$ distributes as shown in Fig. 15, where the distributions on eight sections at $8 \leqslant x/D \leqslant 15$ are plotted. The distribution is nearly in the self-preservation state. When compared with a Gaussian distribution that successfully represents the measured profile, $\overline{\gamma}$ is slightly lower at $1.2 \leqslant r/b_\gamma \leqslant 2.1$ on the sections $x/D \geqslant 13$. This is attributable to the fact that the mean velocity is slightly higher in the jet periphery, as shown in Fig. 9.

Fig. 16 presents the radial distribution for the fluctuation intensity of concentration, r.m.s. γ', where the intensity is nondimensionalized with the value on the jet centerline. The intensity becomes lower with increase in the axial distance x

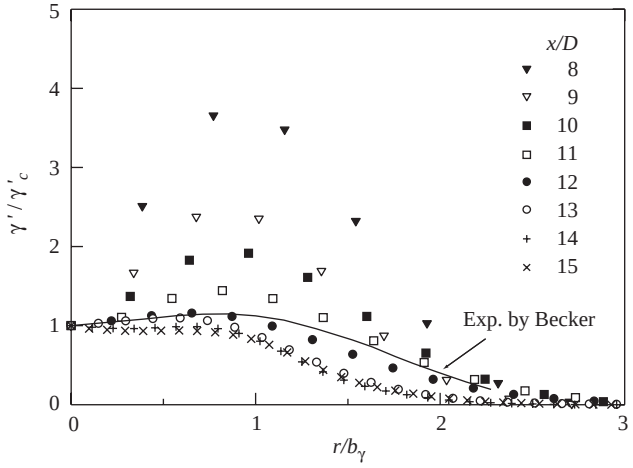

Fig. 16. Radial profile of r.m.s. concentration fluctuation.

at $r/b_\gamma \leqslant 2$, and it tends to approach a self-preservation state at the sections $x/D \geqslant 13$. According to the experiment by Becker et al. (1967), the fluctuation intensity is in the self-preservation state at $x/D \geqslant 20$. The present numerical result is found to successfully represent the experimental trend at $x/D \geqslant 13$. But, it is slightly lower than the measurement at $0.9 \leqslant r/b_\gamma \leqslant 2.3$. This may be because the turbulent intensity chiefly governing the concentration fluctuation does not exactly agree with the measured result.

5. Conclusions

A three-dimensional particle method for the diffusion of matter in a round jet was proposed. The flow field is computed by the vortex method, while the concentration field is simulated through a method analogous to the vortex method. The present method needs no computational grids, because the Lagrangian approach is employed.

The method was applied to the simulation of the diffusion of matter in a compound round jet so as to demonstrate its applicability. The results are summarized as follows:

(1). The large-scale eddies, appearing just downstream of the disappearing point of the potential core, cause the diffusion of matter to the radial direction. In the subsequent developed region of the velocity field, the diffusion proceeds to the smaller vortical structure. These favorably compare with the corresponding experimental results.

(2). The above-mentioned dependence of the diffusion phenomena on the vortical structure is confirmed by investigating the variation of the concentration probability density function along the jet centerline.

(3). The mean concentration and the concentration fluctuation intensity are in the self-preservation state at $x/D \geqslant 8$ and $x/D \geqslant 13$, respectively, suggesting the validity of the present numerical method.

Notation

b_u, b_γ	half-width for velocity and concentration
D	nozzle diameter
$\boldsymbol{l}$	length vector of vortex elements
N_c	number of concentration elements
N_v	number of vortex elements
r	radial coordinate
t	time
t^*	nondimensional time $= U_0 t/D$
U	mean velocity
$\boldsymbol{u}$	velocity
u'	axial velocity fluctuation intensity
$\boldsymbol{x}$	position vector

Greek letters

$\boldsymbol{\alpha}$	strength of vorticity
γ	concentration
γ'	concentration fluctuation intensity
Γ	circulation
ε	core radius of concentration element
δv	volume of vortex element
Δt	time increment
Δt_v	time interval to release vortex element
Δt_c	time interval to release concentration element
κ	diffusivity
ν	kinematic viscosity
σ	core radius of vortex element
$\boldsymbol{\omega}$	vorticity $= \nabla \times \boldsymbol{u}$

Subscripts

a	uniform flow
c	jet centerline
0	nozzle exit

References

Antonia, R.A., Bilger, R.W., 1973. An experimental investigation of an axisymmetric jet in a co-flowing air stream. Journal of Fluid Mechanics 61, 805–822.

Becker, H.A., Hottel, H.C., Williams, G.C., 1967. The nozzle-fluid concentration field of the round, turbulent free jet. Journal of Fluid Mechanics 30, 285–303.

Breidenthal, R., 1981. Structure in turbulent mixing layers and wakes using a chemical reaction. Journal of Fluid Mechanics 109, 1–24.

Cook, A.W., Riley, J.J., 1994. A subgrid model for equilibrium chemistry in turbulent flows. Physics of Fluids 6 (8), 2868–2870.

Forstall, W., Shapiro, A.H., 1950. Momentum and mass transfer in coaxial gas jets. Transactions of ASME Journal of Applied Mechanics 17, 399–408.

Hasegawa, T., Yamaguchi, S., Amano, T., Kagami, T., 1991. Sequential two-dimensional concentration measurement of a cylindrical jet by planar laser scattering method. Transactions of JSME B57 (538), 2060–2064 (in Japanese).

Hockney, R.W., Eastwood, J.W., 1985. Computer Simulation Using Particles, McGraw-Hill, New York.

Kamemoto, K., Miyasaka, T., 2000. Development of a vortex and heat elements method and its application to analysis of unsteady heat transfer around a circular cylinder in a uniform flow. In: Kamemoto, K., Tsutahara, M. (Eds.), Vortex Methods. World Scientific, Singapore, pp. 135–144.

Leonard, A., 1980. Vortex methods for flow simulation. Journal of Computational Physics 37, 289–335.

Ogami, Y., 2001. Simulation of heat-fluid dynamic motion by the vortex method. JSME International Journal B44 (4), 513–519.

Otsuki, H., Murakami, K., Uchiyama, T., 2002. Particle simulation for diffusion of matter in plane mixing layer. Proceedings of the 5th JSME-KSME Fluids Engineering Conference, Nagoya, (on CD-ROM).

Riley, J.J., Metcalfe, R.W., 1985. Direct numerical simulations of chemically reacting turbulent mixing layers. AIAA Paper 85-0321.

Takeuchi, S. Miyake, Y., Kajishima, T., 1999. On the numerical simulation of round jets of incompressible fluid. Proceedings of the 3rd ASME-JSME Joint Fluid Engineering Conference FEDSM99-6957, (on CD-ROM).

Uchiyama, T., 2003. Numerical prediction of the round jet in a co-flowing stream by three-dimensional vortex method. International Journal of Turbo and Jet Engines 20 (3), 235–244.

Uchiyama, T., 2004. Numerical analysis of particulate jet generated by free falling particles. Powder Technology 145, 123–130.

Uchiyama, T., Naruse, M., 2001. A numerical method for gas-solid two-phase free turbulent flow using a vortex method. Powder Technology 119, 206–214.

Uchiyama, T., Naruse, M., 2002. Numerical simulation of gas-particle two-phase mixing layer by vortex method. Powder Technology 125, 111–121.

Uchiyama, T., Naruse, M., 2003. Vortex simulation of slit nozzle gas-solid two-phase jet. Powder Technology 131, 156–165.

Uchiyama, T., Okita, T., 2003. Numerical prediction of plume diffusion field around a circular cylinder by particle method. Advances in Environmental Research 7, 573–581.

Uchiyama, T., Yagami, H., 2003. Numerical simulation of wake gas flow laden with solid particles. Proceedings of the 2nd Asian Particle Technology Symposium, Penang, (on CD-ROM).

Uchiyama, T., Arai, H., Naruse, M., 2000. Numerical study on solid-liquid two-phase flow around a circular cylinder using a vortex method. Proceedings of the 1st Asian Particle Technological Symposium, Bangkok, (on CD-ROM).

Winckelmans, G.S., Leonard, A., 1993. Contribution to vortex particle methods for the computation of three-dimensional incompressible unsteady flows. Journal of Computational Physics 109, 247–273.

Yamashita, H., Kushida, G., Takeno, T., 1996. An experimental study on transition and mixing processes in a coaxial jet. Atlas of Visualization II, 53–66.

Yuu, S., Nishioka, T., Umekage, T., 1990. Direct numerical simulation of three-dimensional Navier–Stokes equations for slit nozzle free jets and experimental verification (1st report, velocity vector diagrams and mean velocity distributions). Transactions of JSME B56 (528), 2239–2246.